Structures 67 (2024) 107033

Contents lists available at ScienceDirect

Structures

journal homepage: www.elsevier.com/locate/structures

An integrated design approach using shape and topology optimization to mitigate climate impact and enhance buildability

Saaranya Kumar Dasari [a,*], Patrizia Trovalusci [a], Nicholas Fantuzzi [b], Marco Pingaro [a], Roberto Panei [c]

[a] DISG Department, Sapienza University of Rome, Via Antonio Gramsci, 53, Rome, 00197, Italy
[b] DICAM Department, University of Bologna, 40126, Bologna, Italy
[c] Municipal Urban Hygiene Company(AMA), Rome, Italy

ARTICLE INFO

Keywords:
Structural optimization
Sustainability
Buildability
Global warming potential

ABSTRACT

In a world where the construction industry is increasingly under the spotlight for its environmental impact, the demand for innovative design approaches has reached unprecedented levels. In response, this paper introduces an innovative design methodology that combines shape and topology optimization, with a focus on mitigating climate change and enhancing buildability, in the context of shell structures. Shape optimization typically involves refining existing designs, while topology optimization focuses on identifying optimal material layouts. Our methodology synergizes these two approaches, enabling the optimization of shape and material distribution, while considering Global Warming Potential and Buildability. This research contributes to advancing the ongoing transformation in spatial structures by topology informed shell structures, emphasizing the environmental challenges.

1. Introduction

The construction industry's contribution to global carbon emissions and resource depletion is undeniable, causing a fundamental shift towards sustainable practices. Traditional construction methods often lead to overuse of materials, and high environmental footprints. To address these issues, an integrated design approach using shape and topology optimization has gained prominence [1,2]. As the demand for sustainable construction practices intensifies, integrated approaches emerge not only as a means to enhance material efficiency but also as a response to the growing need for environmentally conscious design strategies. In the context of spatial structures, the intricate relationship between form and structure is particularly pronounced when dealing with thin shell structures and the shape of the shell is intrinsically tied to the distribution of forces and vice versa. Consequently, designing thin shell structures often involves a two-step process. In the initial phase, form-finding methods are employed to establish the equilibrium shape of the shell. Subsequently, material properties and material distribution are introduced into the numerical model for a detailed structural analysis [3,4]. This research advances our understanding of form-finding and material distribution in shell design. It explores various numerical methods used to determine the equilibrium shape of these structures.

Shape optimization and topology optimization are crucial research domains within shell structure design, encompassing various methodologies. In previous studies, researchers have delved into both in-plane and out-of-plane optimization approaches, with a key distinction being whether shell surface curvatures are allowed to change during the optimization process. Ansola et al. [5] introduced a method for optimizing shell structures that combined shape and topology optimization. In their approach, these optimization steps were performed alternately, with the shell geometry and topology variables optimized sequentially until convergence was achieved. Hassani et al. [6] achieved concurrent shape and topology optimization of shell structures by optimizing both types of design parameters simultaneously in each iteration. Jiang et al. [7] devised an explicit optimization approach based on the moving morphable component method for shell structures, enabling simultaneous optimization. However, most of these methods were not developed for architectural design, where shape is typically predefined. When finding the topology of a shell, the decision between utilizing stiffeners like ribbed structures or opting for high-strength materials in particular areas hold significant importance. Our investigation builds upon this notion by developing an integrated approach where shape and topology optimization steps are conducted subsequently using Dynamic Relaxation (DR) and Solid Isotropic Material with Penalization

* Corresponding author.
E-mail address: saaranyakumar.dasari@uniroma1.it (S.K. Dasari).

https://doi.org/10.1016/j.istruc.2024.107033
Received 15 December 2023; Received in revised form 15 July 2024; Accepted 2 August 2024
Available online 9 August 2024

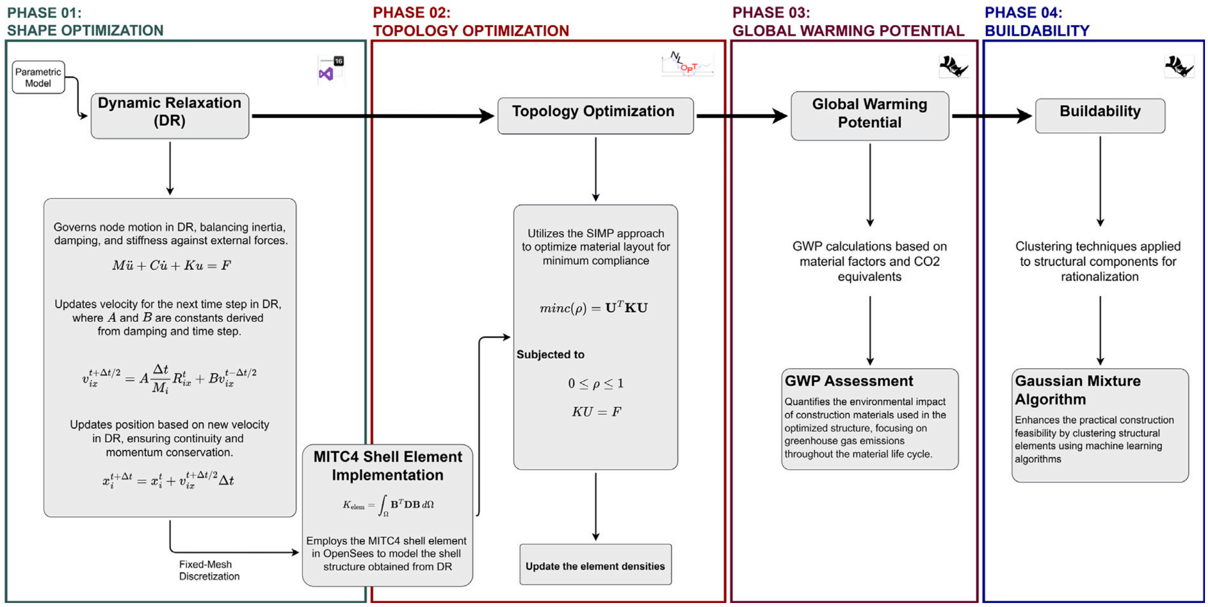

Fig. 1. Sequential steps in the integrated optimization methodology.

(SIMP) methods. To address this challenge, we employed the Method of Moving Asymptotes (MMA) algorithm [8], which utilizes information from design sensitivity analysis, distinguishing our work from previous methods proposed.

An integral aspect of this research is the pivotal role of optimization in shell design. Thin shell structures are often subject to multiple design criteria beyond self-weight support. Therefore, optimization methods emerge as critical tools for achieving design objectives, whether it is about minimizing material usage, reducing weight, managing costs, or maximizing stiffness [9,10]. These objectives are pursued while adhering to specific design constraints, giving rise to multi-objective optimization challenges. It is worth noting that while this research acknowledges the importance of these constraints, the primary focus remains on form-finding and topology optimization techniques, as the application of other constraints lies beyond the immediate scope of this study. Considering the historical construction challenges posed by continuous shell structures, our research ventures into the realms of Environment and Buildability constraints [11]. This method focuses on reshaping the built environment by minimizing environmental impact and improving buildability concurrently. Additionally, the legacy of influential figures such as Antoni Gaudi, Sergio Musmeci, Heinz Isler, Pier Luigi Nervi, and Frei Otto illustrates the fascinating evolution of shape-resistant structures. Their work, alongside research into physical models and the structural optimization of intricate structures like membranes, shells, and grid shells, provides a rich historical backdrop to our research.

The construction challenges encountered in notable projects such as ‘Los Manantiales’ Restaurant in Xochimilco, Mexico (1958) and in the (Meiso no Mori) Crematorium of Kakamigahara, Japan (2006) shine a spotlight on the complexities of thin, continuous shell structures. Initially, these projects embraced a cost-effective approach involving timber custom-built formwork, followed by concrete construction. This method, once perceived as cost-effective due to low labor costs and its alignment with simultaneously balancing forces during construction, began to wane in popularity. Surprisingly, the construction process has seen little evolution over the past 50 years which led to escalation of costs associated with the construction of shell structures. The decline of monolithic reinforced concrete and masonry shells from the 1970s onward was attributed to factors such as escalating labor costs, inefficiencies in on-site fabrication, and the complications associated with customized reinforcement for concrete shells [12]. These practical challenges gradually eroded architects’ enthusiasm for reinforced concrete shells. Consequently, grid shells, featuring cost-efficient lattice systems covered by planar glass or metal panes, ascended as the preferred structural choice for large-span, form-passive surface structures. The dominance of grid shells, however, ushered in concerns regarding the limitations of continuous shell structures.

Fortunately, the 1990s witnessed a technological renaissance marked by the advent of digital design, simulation, and fabrication. This transformative era introduced Computer-Aided-Design (CAD), Computer-Aided-Engineering (CAE), Computer-Aided-Manufacturing (CAM), and industrial robotics, laying the groundwork for an innovative concept known as segmentation [13,14]. However, the current gap between sophisticated software models and the ability to realize designs within reasonable budgets remains a significant obstacle in structural architecture design. Bridging this gap requires consideration of Global Warming Potential (GWP) and Buildability in the design process. The integrated optimization system unveiled in this study signifies a revolutionary approach to determining the optimal form and topology of shell structures. In our methodology, DR is utilized for shape optimization, where a network of vertices undergoes relaxation to form a free-form shape. This process involves constructing a mesh from vertices and edges, which is then converted into shell elements. Subsequently, topology optimization is applied to this shell structure, systematically refining the material distribution to optimize structural performance while minimizing material usage. These structures present unique optimization challenges due to the profound influence of their curvature on stiffness, rendering it inherently complex to predict the ideal design. Additionally, the methodology incorporates assessments of GWP, evaluating the environmental impact through lifecycle analysis of the materials used, aiming to quantify and mitigate the carbon footprint associated with construction. Buildability is also a core focus, employing clustering algorithms and advanced fabrication techniques to enhance the practicality and efficiency of construction processes. To provide a clear overview of the methodology’s structured approach, Fig. 1 summarizes the key steps involved.

2. Methodology

We introduce an innovative methodology merging shape and topology optimization within the architectural framework of shell structure engineering. Traditionally, these optimization techniques were treated separately, first seeking an optimal material layout and subsequently refining the shape. Our approach integrates both, allowing the sequential optimization of shape and material distribution. This integrated approach entails the dynamic modification of the shell structure's shape during the optimization process, establishing a variable ground structure for topology optimization [5,7,15]. Shape optimization methods are crucial for addressing complex design challenges in shell structures, determining the optimal form by manipulating the shell's mid-plane geometry [16]. In parallel, topology optimization focuses on enhancing material distribution within the structure, ultimately reducing overall material usage. It identifies areas where material can be eliminated, culminating in resource-efficient spatial structures [6,17]. In our approach, we concentrate on minimizing compliance while adhering to a fixed material volume. It is essential to note that, although there are other alternatives such as ribbed floor systems [18,19], which utilize isostatic stress lines as ribs, and stiffener layout optimization on shells [20], our integrated method stands out as a comprehensive solution that concurrently addresses shape and material distribution challenges for structural performance. Furthermore, the methodology extends beyond structural optimization to incorporate assessments of GWP and buildability considerations, ensuring that the designs achieve environmental sustainability and practical constructability.

2.1. Shape optimization

The structural performance is deeply embedded in the fundamental principle of harnessing geometric intricacies. Shape optimization techniques provides an effective pathway to embody the principle of leveraging geometric complexities. Through the intrinsic properties of geometric arrangements, shape optimization acts as a catalyst for crafting spatial structures that not only showcase structural efficiency but also demonstrate resilience [21]. The overarching goal of shape optimization revolves around determining the optimal form or geometry of a structure aligned with predefined performance criteria. The application of shape optimization algorithms entails utilizing mathematical optimization techniques, ranging from gradient-based methods to evolutionary algorithms. These algorithms work iteratively to update design variables, enhancing the objective function value while adhering to specified constraints. The ultimate objective is to discover the optimal shape that minimizes the objective function. In conjunction with shape optimization, diverse methods find mention in the literature. These include gravity-based or stiffness-based approaches like the force density method, dynamic relaxation, and particle spring systems [22].

Dynamic Relaxation (DR) and Particle-Systems (PS) are dynamic methods essential for constructing physics-based models, focusing on achieving steady-state solutions. They discretize continuous systems into interconnected nodes or particles to explore dynamic behavior. DR, dating back to 1965, uses explicit time integration for solving differential equations, evolving from frame analysis to handling nonlinear equilibrium in structures. It traces node motion through explicit time increments, reaching static equilibrium. In contrast, PS, since 1983, models discrete bodies in computer graphics. It employs particles connected by springs, forming a versatile mass–spring system, adaptable to various time-integration schemes and dynamics for simulations across diverse fields.

2.1.1. Dynamic relaxation

To implement the DR algorithm, we utilized a Python code developed in Visual Studio, facilitated through the use of an open-source code available online [23]. Developed and maintained by the Block Research Group, this code served as a foundational tool within our computational framework, enabling the effective application of DR to model and analyze structural behavior. The code reads an OBJ file exported from CAD, a plain text file format that represents 3D geometry as shown in Fig. 2. It extracts vertex coordinates and connectivity information, creating a mesh representation of the structure. Subsequently, the DR algorithm is applied to this mesh. During the simulation, vertices experience applied loads and gravitational forces, and internal stiffness forces are calculated based on Hooke's law. Through iterative updates using velocity and acceleration calculations, the system progresses towards equilibrium (Fig. 3).

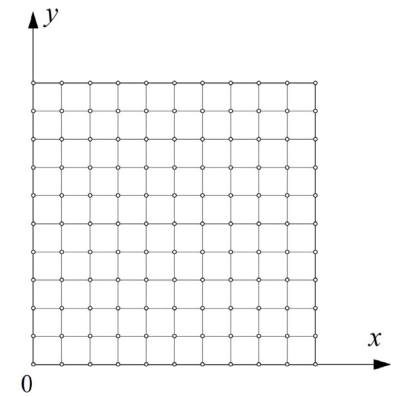

Fig. 2. The initial mesh configuration.

The mathematical foundation of the DR formulation relies on Newton's second law, governing the motion of any node i in the x-direction at time t. This law is applied to calculate the forces acting on each node, including applied forces, gravitational forces, and internal stiffness forces. The equations of motion are iteratively solved using explicit time integration, updating the velocities and positions of the nodes until the system reaches a static equilibrium. The following equations detail the iterative process for accurately modeling the dynamic behavior of the structure and ensuring that the final mesh configuration represents an equilibrium state:

$$M\ddot{u} + C\dot{u} + Ku = F \tag{1}$$

where, M represent the mass matrix, C the damping matrix and K the stiffness matrix. The variables u and its derivatives represent displacement, velocity, and acceleration.

For each coordinate x, y, or z we do the followings:

$$P_{ix} - K_{ix}\delta^t_{ix} - C_i v^t_{ix} = M_i \dot{v}^t_{ix} \tag{2}$$

$$R^t_{ix} = P_{ix} - K_{ix}\delta^t_{ix} = M_i \dot{v}^t_{ix} + C_i v^t_{ix} \tag{3}$$

At node i in direction x at time t, P_{ix} represents the applied force, R^t_{ix} the residual of the applied forces, δ^t_{ix} the total displacement, C_i the viscous damping constant, v^t_{ix} the velocity, M_i indicates the lumped fictitious mass to optimize convergence, and $\dot{v}^t_{ix}$ denotes the acceleration.

Acceleration as an approximate derivative of velocity, it signifies the velocity of a specific moment in time by averaging two half-instances just before and after.

$$\dot{v}^t_{ix} = \frac{v^{t+\Delta t/2}_{ix} - v^{t-\Delta t/2}_{ix}}{\Delta t} \tag{4}$$

$$v^t_{ix} = \frac{v^{t+\Delta t/2}_{ix} + v^{t-\Delta t/2}_{ix}}{\Delta t} \tag{5}$$

By substituting Eqs. (4) and (5) in Eq. (3) and considering that the damping is proportionate to masses $C_i = M_i D$, we have:

$$v^{t+\Delta t/2}_{ix} = A\frac{\Delta t}{M_i} R^t_{ix_i} + B v^{t-\Delta t/2}_{ix} \tag{6}$$

where, $A = (1/1 + D\Delta t)$ and $B = (1 - D\Delta t/1 + D\Delta t)$ and D is constant. Now, we can use the velocities of the nodes to predict the next position in the system.

$$v^{t+\Delta t/2}_{ix} = \frac{x^{t+\Delta t}_i - x^t_i}{\Delta t} \tag{7}$$

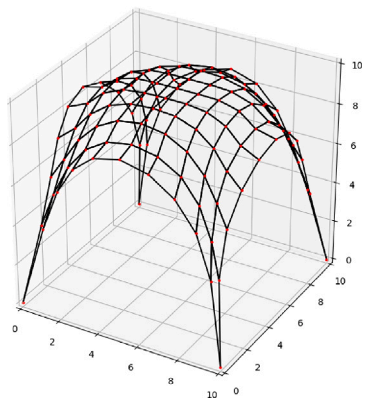

Fig. 3. The final result after applying DR.

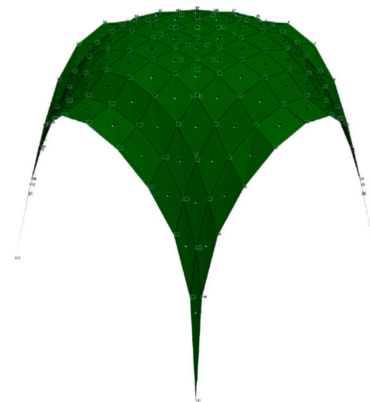

Fig. 4. The MITC4 elements obtained from OpenSees [25].

$$x_i^{t+\Delta t} = x_i^t + v_{ix}^{t+\Delta t/2}\Delta t \quad (8)$$

After obtaining the updated geometry, the new forces can be calculated and integrated with the applied gravity load components P_{ix} to yield the updated residuals.

$$R_{ix}^t = P_{ix} + \sum_{i\ j}\left(\frac{f_{i,j}}{l_{i,j}}\right)^t (x_i - x_j)^t \quad (9)$$

where, t denotes a time step indicator, f_{ij} represents the elasticity force along the edge (i, j), and l_{ij} is the length of that edge. The division by this length in every direction provides the corresponding shadow. The forces along the edges of the mesh are computed with respect to their rest lengths, given by $f_{ij} = K\Delta l$. After computing residual force, updating the velocities and coordinates using Eqs. (7) and (8) we get the final shape as shown in Fig. 3.

The simulation involves various parameters, including the elasticity constant, acceleration damping, time step, and mass. These parameters collectively influence the stiffness, stability, and speed of the simulation. Forces acting on the structure encompass applied loads, gravity, and stiffness forces, contributing to the establishment of an overall equilibrium configuration. The resulting mesh serves as a valuable basis for further analysis, either for optimization purposes or as a starting point for subsequent design iterations.

Fixed-mesh discretization

Following the DR process, the equilibrium shape is discretized into a mesh suitable for further analysis. This involves generating faces and connecting them to form a coherent mesh. The coordinates obtained from DR are structured into a grid, and the faces are defined to facilitate the application of shell elements. Faces are generated by grouping every four adjacent nodes into a quadrilateral element, ensuring that the mesh accurately represents the geometric domain of the structure. The mesh is constructed using face arrays and vertex arrays obtained from the DR process. This fixed-mesh discretization ensures that the structural geometry is accurately represented, allowing for precise application of loads and boundary conditions in the subsequent optimization steps.

2.1.2. The MITC shell element

The MITC4 (Mixed Interpolation of Tensorial Components) shell element is utilized for structural analysis due to its accuracy in capturing both bending and membrane behaviors [24]. The element is quadrilateral, constructed from four nodes, and acts primarily as a membrane with midsurface properties. The MITC4 elements provide a reliable means of modeling thin shell structures, combining mixed interpolation and geometric flexibility. This technique mitigates issues like shear locking by ensuring accurate interpolation of shear strain components, enhancing the element's performance in bending and membrane actions. Additionally, the element can represent both flat and curved geometries, utilizing the mid-surface geometry, thickness variation, and director vectors to model complex shell structures effectively.

In our study, we implemented the MITC4 element using OpenSees [25], an open-source software framework for structural analysis. The elements were defined with a thickness of $h = 0.05$ m, Young's modulus $E = 200$ GPa, and Poisson's ratio $\nu = 0.3$. The material is specified as an elastic isotropic material, and section properties are defined using the "ElasticMembranePlateSection" command in OpenSees. Finally, the MITC4 shell elements are created using the generated mesh faces, ensuring accurate modeling and foundation for topology optimization Fig. 4.

2.2. Topology optimization

Topology optimization entails the generation of an optimal structural layout within the design space. It involves the manipulation of the connectivity between material domains within the structure [26]. We employ material formulation to elucidate the structural layout, enabling the separation or integration of material domains. The optimization problem is typically expressed through material density variables, with '1' denoting material presence and '0' representing void regions [27]. The Solid Isotropic Material with Penalization (SIMP) method formulates topology optimization as a material distribution problem, where the design domain is divided into finite elements. At the material level involves Plane Strain (Stress) elasticity with a constant Poisson ratio and Young modulus interpolated between full material and void, facilitated by a scalar variable [28]. Each element is assigned a design variable denoting the material density, which represents the volume fraction of material in that element. SIMP method is based on penalization techniques. It assigns continuous material densities to each element in the design domain and penalizes intermediate densities to encourage either fully dense (solid) or void (empty) regions. By iteratively adjusting the penalization parameter, SIMP optimizes the material distribution by either including or excluding elements based on their densities [29–31].

In SIMP topology optimization, various methods, including the MMA, Optimal Criteria (OC) Methods, and Level Set Methods, can be employed to iteratively enhance the design. These methods are not mutually exclusive, and their combinations or variations can be applied based on specific optimization requirements. MMA [8], for example, utilizes approximations to true constraint functions and solves subproblems to find feasible and optimal solutions, particularly effective for large-scale optimization problems.

To implement topology optimization techniques, Python code in Visual Studio was employed. This code is based on Ole Sigmund's work

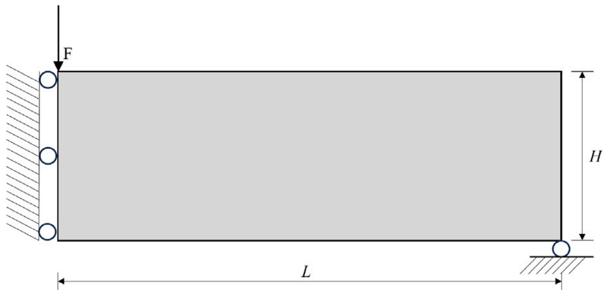

Fig. 5. Design space of MMB beam.

and its extensions from existing literature [32]. Leveraging the SIMP method, MMA algorithm, and gaussian filters, these codes simplify the implementation of the algorithm by incorporating the NLopt [33] and autograd [34] Python libraries.

The considered structure is a standard MMB beam [32]. In Fig. 5, the large gray rectangle represents the design space. To maintain symmetry, our optimization focuses on half of the beam, intending to mirror the results around the left wall. This implies that the beam's center is located on the left side of the illustration. The downward-pointing arrow indicates the application of a load force at this center, while horizontally fixed points represent forces transmitted from the other half of the beam. Additionally, the vertically fixed point in the bottom right corner signifies a normal force from an external support, possibly the top of a wall.

Assuming a rectangular design domain, we discretize it with square elements, each having four nodes per element and two degrees of freedom (DOFs) per node. Node and element numbering proceeds from left to right, with DOFs 2n-1 and 2n corresponding to horizontal and vertical displacements of node n. This regular mesh structure offers opportunities for computational efficiency during the optimization loop. The finite element pre-processing stage begins with defining material properties. We adopted the modified SIMP method from [32]. In this method, each element e is given a density ρ_e that dictates its Young's modulus E_e.

The material stiffness $E_e(\rho_e)$ is defined as follows:

$$E_e(\rho_e) = (E_{\min}) + \rho_e^p(E_0 - E_{\min}), \quad \rho_e \in [0,1] \tag{10}$$

Here, E_0 represents the Young's modulus of the material, E_{min} is the artificial Young's modulus assigned to void regions to prevent the stiffness matrix from becoming singular, and p is a penalization factor ($p = 3$). The material stiffness, $E_e(\rho_e)$, is determined by a formula involving E_0, E_{min}, and a variable ρ_e in the range [0, 1]. The objective function aims to minimize the elastic potential energy or compliance of the 2D grid of springs.

$$\min_{\rho} : \quad c(\rho) = \mathbf{U}^T\mathbf{K}\mathbf{U} = \sum_{e=1}^{N} E_e(\rho_e)\mathbf{u}_e^T\mathbf{k}_0\mathbf{u}_e \tag{11}$$

$$\text{Subjected to :} \quad \begin{array}{c} 0 \le \rho \le 1 \\ \mathbf{K}\mathbf{U} = \mathbf{F} \end{array} \tag{12}$$

In this context, c is compliance and ρ is a vector that represents the material densities of the elements. The compliance is expressed as $\mathbf{U}^T\mathbf{K}\mathbf{U}$, where $\mathbf{U}$ is a vector containing node displacements, $\mathbf{K}$ is the global stiffness matrix, and E_e is Young's modulus. External forces are represented by the vector $\mathbf{F}$, the element displacement vector is represented by $\mathbf{u}_e$, $\mathbf{k}_0$ is the element stiffness matrix for an element and N represents the number of elements used to discretize the design domain. The core objective function, $c(\rho) = \mathbf{U}^T\mathbf{K}\mathbf{U}$, is implemented as a high-level function calling various subroutines.

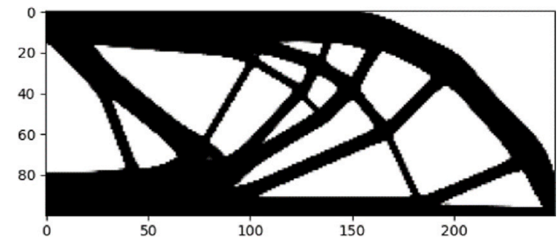

Fig. 6. Optimal layouts of the MMB beam.

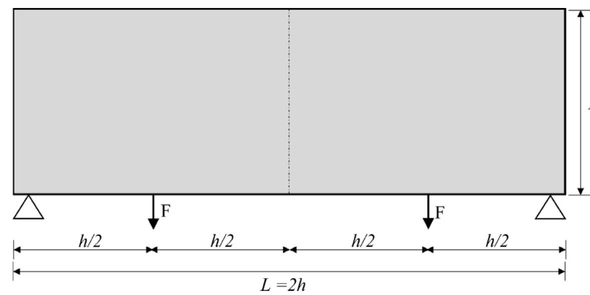

Fig. 7. Simply supported beam loaded with two forces at 1/4 and 3/4 of the span length.

To minimize the objective function $c(\rho)$, we compute the gradients of c with respect to ρ, this allows us to determine the optimal direction for adjusting ρ:

$$\frac{\partial c}{\partial \rho_e} = -p\rho_e^{p-1}(E_0 - E_{min})\mathbf{u}_e^T\mathbf{k}_0\mathbf{u} \tag{13}$$

At a high level, compliance c is given by $\mathbf{U}^T\mathbf{K}\mathbf{U}$. While $\mathbf{U}$ and $\mathbf{K}$ are sparse, making $\sum_{e=1}^{N} E_e(\rho_e)\mathbf{u}_e^T\mathbf{k}_0\mathbf{u}_e$ more efficient, its vectorized implementation might appear complex but significantly speeds up the computation. Element stiffness matrix $\mathbf{k}_0$ is a 2D analogy to the spring constant in a simple harmonic oscillator. Its role is crucial in calculating the potential energy of the system, where $PF = 1/2\mathbf{u}_e^T\mathbf{k}_0\mathbf{u}_e$. Material Constants, Young's modulus and Poisson's coefficient are integral to the element stiffness matrix. These constants play key roles in defining the stiffness and contraction properties of materials, influencing the overall stiffness matrix.

Determining node displacements involves solving the matrix equation $\mathbf{F} = \mathbf{K}\mathbf{U}$ for $\mathbf{U}$. With N nodes and 2 degrees of freedom each, the resulting system of simultaneous linear equations becomes a vital aspect of the problem. As the number of nodes grows, the challenge lies in managing the computational load efficiently. The construction of the global stiffness matrix $\mathbf{K}$ involves dealing with sparse matrices, saving significant memory. The MMA emerges as an effective optimization approach, capable of handling nonlinear inequality constraints and scaling to large parameter spaces. NLopt, coupled with Autograd, facilitates the gradient-based optimization process, particularly suitable for structural optimization problems. Constraints related to mass conservation and density are integrated into the MMA framework for comprehensive optimization. (6) demonstrates outcomes that closely resemble those of foundational work by Ole Sigmund [32], using the SIMP method, MMA algorithm, and gaussian filters, effectively simplifying the optimization process. These tools collectively enhance the code's ability to efficiently solve complex topology optimization problems, aligning closely with established methodologies while ensuring reliable results.

To make the design approach more extensive, we examine an example from [8]. This example involves a ground structure subjected to various mesh sizes and densities. Specifically, the structure, as depicted in Fig. 7, is transmitting two symmetrically located vertical forces to

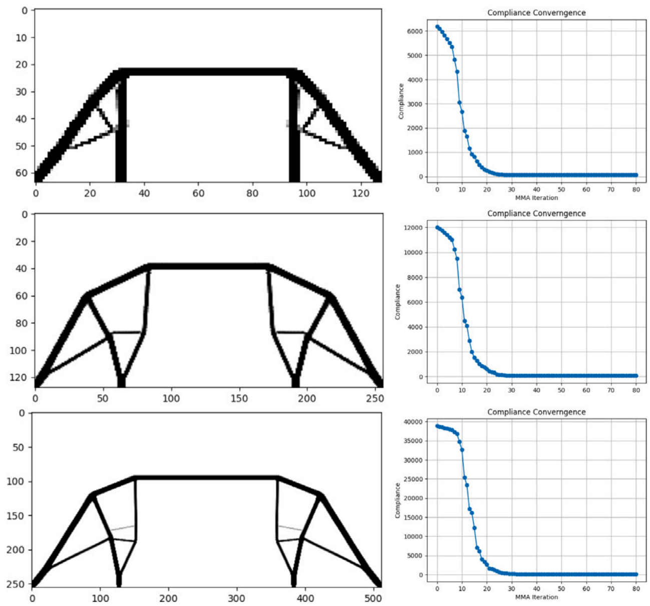

Fig. 8. Mesh density sensitivity: (top) mesh 128 × 64, (middle) 256 × 128, (bottom) 512 × 256. left: results, right: convergence.

fixed supports. The application points of these forces are positioned at 1/4 and 3/4 of the span length. The feasible domain is defined as the half plane over the line. The resulting layouts for different mesh densities are visually represented in Fig. 8.

In our previous study [11], we employed the PS method for shape optimization in Rhino/Grasshopper, utilizing the Kangaroo plugin [22]. Additionally, we conducted topology optimization using the Bi-directional Evolutionary Structural Optimization (BESO) algorithm within the Karamba framework a plugin for Grasshopper. However, the obtained results exhibited inaccuracies attributed to mesh irregularities. Acknowledging this limitation, we embarked on a comprehensive integration of the entire process in Python, combining DR and SIMP. Although this novel implementation is a work in progress and requires further refinement, it represents a significant step towards addressing the inaccuracies observed in the earlier results.

To enhance the accuracy and reliability of our approach, the authors intend to refine and present a fully integrated solution in future research work. The original concept and research framework [5] are visually depicted in Fig. 9(b), providing a conceptual foundation for the ongoing work.

2.2.1. Post processing

After the optimization process, the designed structures are evaluated against GWP and buildability, ensuring that they are prioritized alongside structural performance metrics. In the realm of shell structures, GWP serves as a crucial metric for assessing the environmental impact of the optimized shell structures. The calculations involve quantifying the greenhouse gas emissions associated with the production, transportation, and assembly of construction materials used in the optimized structures. On other hand, segmentation entails breaking down the continuous surface into discrete panels or elements. This process facilitates rationalization, simplification, and standardization of design and construction processes. The integration of optimization and segmentation offers significant potential for enhancing design efficiency and constructability. By incorporating segmentation techniques into the optimization process, designers can optimize not only the overall form and material distribution of the structure but also the layout and arrangement of individual components.

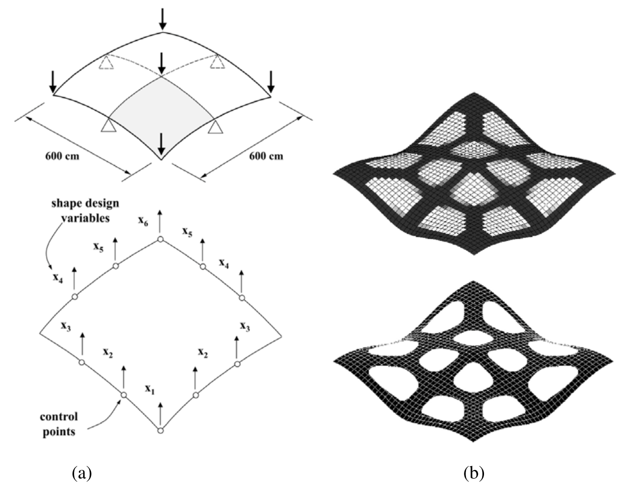

Fig. 9. Original research taken from [5].

2.3. Global warming potential

An integral aspect of our integrated design approach is the incorporation of GWP which serves as a metric that quantifies the structural contribution to greenhouse gas emissions over the entire lifecycle of a construction project. By seamlessly integrating GWP assessment into the design process, we empower designers and stakeholders to make environmentally responsible decisions. This proactive consideration of GWP not only allows for the identification of potential environmental impacts but also facilitates the implementation of strategies to mitigate a project's carbon footprint.

$$\sum \text{structural elements}[\text{Quantity}(\text{kg}) \times \text{CO}_2 e \times \text{material factor}(\text{kgCO}_2 e/\text{kg})] = \text{GWP building}(\text{kgCO}_2 e) \quad (14)$$

When dealing with single-material structures, reducing the volume or weight of the structure can be seen as a means to lessen its environmental footprint. This is because a lighter structure typically entails lower energy consumption and fewer Greenhouse Gas (GHG) emissions during the material production phase. In the context of multi-material structures, simply minimizing structural volume or weight does not necessarily correspond to reducing environmental impact. This is because various materials used in such structures may have different densities, energy intensities, and GHG emission coefficients. Here, the environmental impact of a structure refers to the energy consumption or GHG emissions incurred by the structure over its operational lifespan. Consider, for example, a shell structure derived from DR, constructed from concrete with a thickness of 60 mm. The embodied carbon for this shell is calculated to be 15,714.3475 $kgCO_2e$, using concrete with a GWP of 0.8 $kgCO_2e/kg$ as the material [35]. The Cardinal LCA plugin for Grasshopper was employed to illustrate this in Fig. 10.

2.4. Buildability

Buildability, denoting the ease of construction and the adoption of efficient construction techniques, constitutes another crucial aspect. According to [36] buidability is defined as *the extent to which the design of a building facilitates ease of construction as well as the extent to which the adoption of construction techniques and processes affects the productivity level of building works*. It encompasses how the utilization of construction methods and techniques impacts the efficiency and productivity of construction activities. An optimized design should not only exhibit environmental sustainability but also practical feasibility

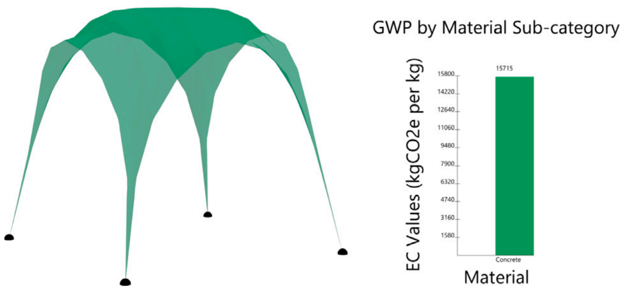

Fig. 10. GWP analysis of the shell obtained from DR.

Fig. 11. Segmentation of the shell obtained from DR.

in construction. By integrating buildability assessments during the design phase, projects can minimize construction delays, cost overruns, and enhance overall operational efficiency.

Rationalization, a principle not confined to architecture but widely applied in construction engineering and product design, has become increasingly important due to the growing complexity of architectural geometries [37]. The advent of computational design tools has enabled architects to conceive intricate geometries, yet realizing these complex shapes remains a challenge. Architects often need to modify designs to align with the constraints of the fabrication process, a process known as architectural rationalization [38]. By rationalizing the design, complex shell geometries can be simplified and optimized for efficient construction. One method to achieve this involves leveraging machine learning algorithms, such as the Gaussian mixture algorithm, to cluster and group the panels of a shell structure.

2.4.1. Clustering

In the realm of machine learning and data analysis, clustering is a foundational technique used to organize unlabeled data points into meaningful collections or clusters based on inherent similarities or shared characteristics. For instance, when analyzing large datasets, clustering helps identify distinct subgroups or patterns, facilitating tasks like customer segmentation, anomaly detection, or recommendation systems. Various clustering algorithms, including K-Means, and Hierarchical Clustering are employed in machine learning for grouping data points based on specific characteristics and objectives [39]. In structural architecture, clustering involves applying data-driven techniques, such as the Gaussian Mixture algorithm, to group structural elements or components based on shared attributes. This clustering approach is particularly useful for rationalization efforts in architectural and structural design, offering several benefits in the construction and fabrication of complex structures.

2.4.2. Gaussian mixture algorithm

Gaussian Panel Groupings, in architectural and structural design, refer to applying the Gaussian Mixture algorithm to organize 3D panel geometries into clusters based on shared dimensional characteristics. This approach supports subsequent design and fabrication activities, especially in the context of shell structures and rationalization efforts. The Gaussian Mixture algorithm, falling under unsupervised learning algorithms, comprehensively analyzes the geometric attributes, dimensions, and connections of individual panels within a shell structure. The algorithm groups these panels into coherent clusters based on inherent similarities, typically starting with subdividing the shell's surface into individual panels (segmentation), which are then organized into clusters. The segmentation of the shell obtained from DR in Fig. 11 involves clustering based on the area of the panels.

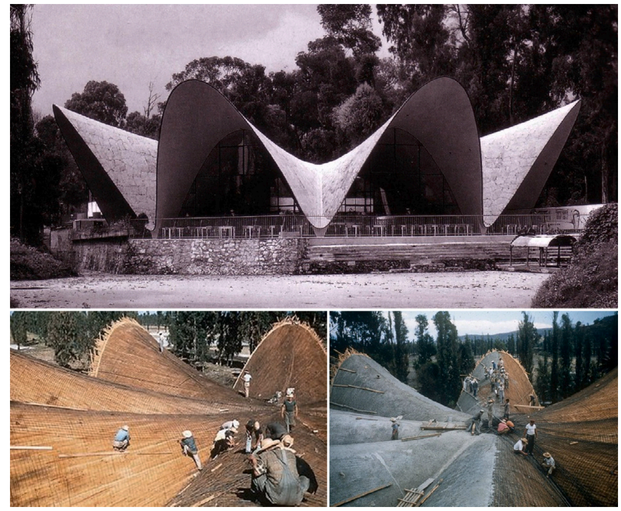

Fig. 12. Los Manantiales' Restaurant in Xochimilco, Mexico (1958).

Fig. 13. Crematorium of Kakamigahara, Japan (2006).

3. Case study

The construction of continuous shell structures, exemplified by the Los Manantiales Restaurant in Xochimilco, Mexico (1958) Fig. 12 and Crematorium of Kakamigahara (Meiso no Mori), Japan (2006) Fig. 13 presents inherent challenges, as highlighted in the introduction. Building these structures, with all their intricate shapes and curves, involves creating precise formwork, which makes the construction process more complicated and expensive.

In this particular instance, the shell's construction involves a two-step process: initially crafted in timber as bespoke formwork and

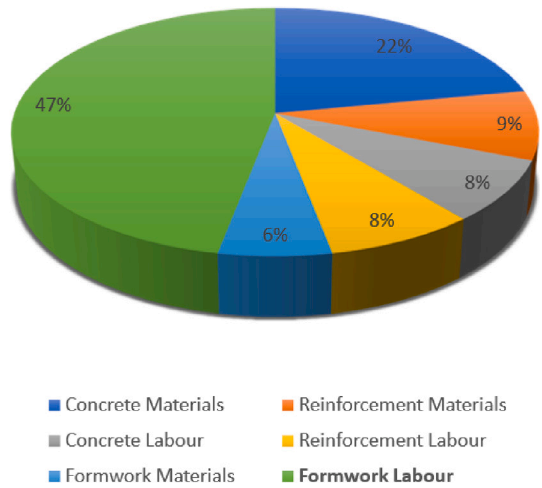

Fig. 14. Cost of Formwork [40].

Fig. 15. GWP of Los Manantiales Restaurant, Mexico (1958).

subsequently replicated in concrete. The design, fabrication, and installation of the formwork demand careful consideration to achieve the intended shape and uphold the structural integrity of the concrete shell. According to [40], the cost linked to formwork constitutes a substantial portion, typically ranging from 40% to 60%, of the total expenses incurred in constructing a concrete structure Fig. 14.

The cost associated with constructing these structures, especially when deploying substantial formwork, stems from various factors. Primarily, significant labor and time investments are required for the creation and assembly of the formwork. Skilled labor is essential for accurately constructing the formwork, given the intricacies of the geometry involved. Furthermore, the materials used in the formwork, such as timber or steel, contribute to the overall expenses. Integrating considerations of buildability and GWP into the design process becomes imperative to mitigate the environmental impact of constructing such structures. Los Manantiales's reinforced concrete shell with a thickness of 40 mm, the total embodied carbon amounts to 4 029 069.31 $kgCO_2e$. This calculation is based on the material concrete, which has a GWP of 0.8 $kgCO_2e/kg$ [35]. To analyze this, we utilized the Cardinal LCA plugin for Grasshopper, employing it to compute the GWP of Los Manantiales Fig. 15 while considering embodied carbon factors from the database [35].

Rationalization in shell structures entails identifying repetitive patterns and standardizing design and fabrication processes. Tools like Lunch Box ML for Grasshopper are often used to facilitate this clustering procedure [41]. The clustering of panels through the Gaussian mixture algorithm provides several advantages in the rationalization of shell structures. It helps reduce the proliferation of unique panel types, establishing standard dimensions and connection details, streamlining the production process, and simplifying fabrication complexities as you can in Fig. 16 the rationalization of Los Manatiales. This leads to cost savings, shorter manufacturing lead times, and more efficient and economical construction practices. Additionally, by capitalizing on the distinct structural properties of materials and aligning them with the topology of the structure, we can strategically allocate materials. This not only optimizes the performance of the structure but also facilitates the easy assembly and transportation of prefabricated panels. Such a strategic approach enhances efficiency throughout the construction process.

Fig. 16. Rationalization of Los Manantiales.

Moreover, panel clustering aids in the management and organization of components during transportation and installation, mitigating logistical challenges and enhancing ease of handling during construction. This comprehensive approach addresses not only the architectural intricacies of shell structures but also emphasizes environmental sustainability and cost-effectiveness, contributing significantly to the evolution of construction practices. Future case studies and in-depth analyses could further enrich our understanding and application of these integrated design methodologies.

4. Final remarks

This paper presents an integrated design approach that combines shape and topology optimization to improve the sustainability and buildability of shell structures by addressing GWP. The integration of shape and topology optimization is achieved through an iterative framework. Initially, Dynamic Relaxation(DR) is used to optimize the shape of the shell structure. The resulting equilibrium geometry is then discretized into a mesh for topology optimization. The shape obtained from DR enables the construction of a mesh with faces and updates coordinates, followed by constructing MITC4 shell elements using OpenSees. This method ensures accurate simulation while seamlessly accommodating the sequence of optimization. By integrating Solid Isotropic Material with Penalization (SIMP) and utilizing the Moving Asymptotes with the NLopt library, our approach optimizes both form and material distribution within shell structures. The combined approach leverages the strengths of both optimization techniques, ensuring that the final design is optimized in terms of both geometry and material usage. This optimization leads to a significant reduction in material usage, which directly contributes to mitigating climate impact by lowering the carbon footprint associated with material production and transportation. Incorporating GWP assessments addresses environmental concerns, making the design process more eco-friendly. Design rationalization techniques, including machine learning algorithms, streamline construction processes and improve buildability. This approach minimizes the need for precise scaffolding, allowing for prefabrication of components, which simplifies construction and reduces on-site labor and waste. Future work could include detailed case studies and expanded optimization criteria to further validate and refine the approach. Although our approach requires further refinement and development, it holds potential for sustainable practices in the construction industry, particularly in spatial structures.

CRediT authorship contribution statement

Saaranya Kumar Dasari: Conceptualization, Data curation, Formal analysis, Investigation, Methodology, Software, Validation, Visualization, Writing – original draft, Writing – review & editing. **Patrizia Trovalusci:** Funding acquisition, Project administration, Resources, Supervision, Writing – review & editing. **Nicholas Fantuzzi:** Conceptualization, Methodology, Project administration, Resources, Supervision, Validation, Writing – review & editing. **Marco Pingaro:** Conceptualization, Methodology, Supervision, Validation, Writing – review & editing. **Roberto Panei:** Conceptualization, Methodology, Supervision, Writing – review & editing.

Declaration of competing interest

The authors declare that they have no known competing financial interests or personal relationships that could have appeared to influence the work reported in this paper.

Acknowledgments

The Authors gratefully acknowledge the financial support provided by the Italian Ministry of University and Research P.N.R.R. National Grant No. PNRR- CN1- Spoke6- (B83C22002940006) and the PhD program of Structural and Geotechnical Engineering, Sapienza University of Rome, Italy.

References

[1] Cai S, Zhang H, Zhang W. An integrated design approach for simultaneous shape and topology optimization of shell structures. Comput Methods Appl Mech Engrg 2023;415:116218. http://dx.doi.org/10.1016/j.cma.2023.116218.

[2] Ho-Nguyen-Tan H-GK. An efficient method for shape and topology optimization of shell structures. Struct Multidiscip Optim 2022;65. http://dx.doi.org/10.1007/s00158-022-03213-0.

[3] Dasari SK, Fantuzzi N, Trovalusci P, Panei R, Pingaro M. Optimal design of a canopy using parametric structural design and a genetic algorithm. Symmetry 2023;15(1). http://dx.doi.org/10.3390/sym15010142.

[4] Dasari SK, Fantuzzi N, Trovalusci P, Panei R. Computational approach for form-finding optimal design. Archit Struct Constr 2022;2(3). http://dx.doi.org/10.1007/s44150-022-00077-2.

[5] Ansola R, Canales J, Tárrago JA, Rasmussen J. An integrated approach for shape and topology optimization of shell structures. Comput Struct 2002;80(5):449–58. http://dx.doi.org/10.1016/S0045-7949(02)00019-6.

[6] Behrooz H, Mehdi TS, Hossein G. Simultaneous shape and topology optimization of shell structures. Struct Multidiscip Optim 2013;48:221–33. http://dx.doi.org/10.1007/s00158-013-0894-9.

[7] Jiang X, Zhang W, Liu C, Du Z, Guo X. An explicit approach for simultaneous shape and topology optimization of shell structures. Appl Math Model 2023;113:613–39. http://dx.doi.org/10.1016/j.apm.2022.09.028.

[8] Svanberg K. The method of moving asymptotes—a new method for structural optimization. Internat J Numer Methods Engrg 1987;24(2):359–73. http://dx.doi.org/10.1002/nme.1620240207.

[9] Benvenuto E. An introduction to the history of structural mechanics. 3rd ed.. New York: Springer-Verlag; 1991.

[10] Kirsch U. Optimum structural design. New York: McGraw-Hill; 1981.

[11] Dasari SK, Trovalusci P, Fantuzzi N, Pingaro M, Panei R. Sustainable spatial structures: A design approach using shape and topology optimization to minimize environmental impact and improve buildability. In: Gabriele S, Manuello Bertetto A, Marmo F, Micheletti A, editors. Shell and spatial structures. Cham: Springer Nature Switzerland; 2024, p. 279–88.

[12] Sigrid A, Philippe B, Diederik W. Shell structures for architecture: form finding and optimization. London: Routledge; 2014, http://dx.doi.org/10.4324/9781315849270.

[13] Pottmann H, Eigensatz M, Vaxman A, Wallner J. Architectural geometry. Comput Graph 2015;47(C):145–64. http://dx.doi.org/10.1016/j.cag.2014.11.002.

[14] Slawomir Koziel X-SY. Computational optimization, methods and algorithms. Heidelberg: Springer Berlin; 2016, http://dx.doi.org/10.1007/978-3-642-20859-1.

[15] Christiansen AN, Bærentzen JA, Nobel-Jørgensen M, Aage N, Sigmund O. Combined shape and topology optimization of 3D structures. Comput Graph 2015;46:25–35. http://dx.doi.org/10.1016/j.cag.2014.09.021, Shape Modeling International 2014.

[16] Barnes MR. Form finding and analysis of tension structures by dynamic relaxation. Int J Space Struct 1999;14(2):89–104. http://dx.doi.org/10.1260/0266351991494722.

[17] Ansola R, Canales J, Tárrago JA, Rasmussen J. Combined shape and reinforcement layout optimization of shell structures. Struct Multidiscip Optim 2004;27:219–27. http://dx.doi.org/10.1007/s00158-004-0399-7.

[18] Veenendaal D, Bakker J, Block P. Structural design of the flexibly formed, mesh-reinforced concrete sandwich shell roof of NEST HiLo. J Int Assoc Shell Spatial Struct 2017;58(1):23–38. http://dx.doi.org/10.20898/j.iass.2017.191.847.

[19] Halpern AB, Billington DP, Adriaenssens S. The ribbed floor slab systems of pier luigi nervi. In: Proceedings of IASS annual symposia. no. 23, International Association for Shell and Spatial Structures (IASS); 2013, p. 1–7.

[20] Feng S, Zhang W, Meng L, Xu Z, Chen L. Stiffener layout optimization of shell structures with B-spline parameterization method. Struct Multidiscip Optim 2021;63:2637–51.

[21] Bletzinger K-U, Wüchner R, Daoud F, Camprubí N. Computational methods for form finding and optimization of shells and membranes. Comput Methods Appl Mech Engrg 2005;194(30):3438–52. http://dx.doi.org/10.1016/j.cma.2004.12.026, Structural and Design Optimization.

[22] Piker D. Kangaroo: Form finding with computational physics. Archit Des 2013;83(2):136–7. http://dx.doi.org/10.1002/ad.1569.

[23] Mele TV. Dynamic relaxation. 2023, https://block.arch.ethz.ch/blog/2014/07/dynamic-relaxation/. [Accessed June 2023].

[24] Dvorkin EN, Bathe K-J. A continuum mechanics based four-node shell element for general non-linear analysis. Eng Comput 1984;1(1):77–88.

[25] Mazzoni S, McKenna F, Scott MH, Fenves GL. OpenSees command language manual. 2006, https://openseespydoc.readthedocs.io/en/latest/index.html.

[26] Deaton JD, Grandhi RV. A survey of structural and multidisciplinary continuum topology optimization: post 2000. Struct Multidiscip Optim 2014;49:1–38.

[27] Woldseth RV, Aage N, Bærentzen JA, Sigmund O. On the use of artificial neural networks in topology optimisation. Struct Multidiscip Optim 2022;65(10):294.

[28] Bendsøe MP, Sigmund O. Topology optimization. Heidelberg: Springer Berlin; 2002, http://dx.doi.org/10.1007/978-3-662-05086-6.

[29] Sigmund O, Maute K. Topology optimization approaches: A comparative review. Struct Multidiscip Optim 2013;48(6):1031–55.

[30] Song Y, Ma Q, He Y, Zhou M, Wang MY. Stress-based shape and topology optimization with cellular level set in B-splines. Struct Multidiscip Optim 2020;62:2391–407.

[31] Hoyer S, Sohl-Dickstein J, Greydanus S. Neural reparameterization improves structural optimization. 2019, http://dx.doi.org/10.48550/arXiv.1909.04240.

[32] Andreassen E, Clausen A, Schevenels M, Lazarov BS, Sigmund O. Efficient topology optimization in MATLAB using 88 lines of code. Struct Multidiscip Optim 2011;43:1–16.

[33] Johnson SG. The NLopt nonlinear-optimization package. 2007, https://github.com/stevengj/nlopt.

[34] Maclaurin D, Duvenaud D, Adams RP. Autograd: Effortless gradients in numpy. In: ICML 2015 autoML workshop. Vol. 238, 2015, p. 5.

[35] Embodied carbon footprint database -circular ecology. 2023, https://circularecology.com. [Accessed June 2023].

[36] BCA,: Code of practice on buildability 2022 edition, 1–105. 2023, https://www1.bca.gov.sg. [Accessed May 2023].

[37] Liu Y, Lee T-U, Javan AR, Pietroni N, Xie YM. Reducing the number of different faces in free-form surface approximations through clustering and optimization. Comput Aided Des 2023;166:103633. http://dx.doi.org/10.1016/j.cad.2023.103633.

[38] Pellis D, Kilian M, Pottmann H, Pauly M. Computational design of Weingarten surfaces. ACM Trans Graph 2021;40(4):1–11.

[39] Bhimani J, Leeser M, Mi N. Accelerating K-means clustering with parallel implementations and GPU computing. In: 2015 IEEE high performance extreme computing conference. HPEC, IEEE; 2015, p. 1–6. http://dx.doi.org/10.1109/HPEC.2015.7322467.

[40] Robert H, Lab Jr P. Think formwork – reduce costs. 2007, https://www.structuremag.org/?p=6141.

[41] Miller N, Stasiuk D. Negotiating structured building information data. In: Design transactions: rethinking information modelling for a new material age. 2020, p. 68–73.